Post-print of: Siebert A., Cholewiński G., Garwolińska D., Olejnik A., Rachoń J., Chojnacki J.: The synthesis and structure of a potential immunosuppressant: N-mycophenoyl malonic acid dimethyl ester. JOURNAL OF MOLECULAR STRUCTURE. Vol. 1151, (2018), s. 218-222. DOI: 10.1016/j.molstruc.2017.09.041

# The synthesis and structure of a potential immunosuppressant: N-mycophenoyl malonic acid dimethyl ester

Agnieszka Siebert [a], Grzegorz Cholewiński [a], Dorota Garwolińska [a], Adrian Olejnik [b], Janusz Rachoń [a], Jarosław Chojnacki [b]

[a] Department of Organic Chemistry, Gdansk University of Technology, G. Narutowicza 11/12, Gdansk, PL-80233, Poland [b] Department of Inorganic Chemistry, Gdansk University of Technology, G. Narutowicza 11/12, Gdansk, PL-80233, Poland

**a b s t r a c t**

The synthesis of a potential immunosuppressant, i.e. dimethyl ester of N-mycophenoyl malonic acid was optimized in the reaction of mycophenolic acid (MPA) with amino malonic dimethyl ester in the pres-ence of propanephosphonic anhydride (T3P) as a coupling reagent. The structural properties of the obtained MPA derivative were investigated by NMR, MS and single crystal X-ray diffraction methods. Theoretical considerations of conformational flexibility based on DFT calculations are presented.

Keywords: Crystal structure, Mycophenolic acid, Amide, Immunosuppressants, InChIKey: LWYWUEPXPWSLEA-UHFFFAOYSA-N

## 1. Introduction

Mycophenolic acid **1** (MPA) is a potent inosine 5′-monophosphate dehydrogenase (IMPDH) inhibitor which possesses immunosuppressive properties. Due to their immunosuppressive characteristics, both MPA derivatives, namely, mycophenolate sodium (MPS, Myfortic) and mycophenolate mofetil (MMF, CellCept) are used in medicine to prevent organ transplant rejection and to treat autoimmune disorders [1] [2], [3]. The optimization of the synthesis of MPA molecule-based active substance included the synthesis of numerous MPA derivatives (see Refs. [4] [5], [6] [7], [8]) due to the fact that several structural features are crucial for maintaining the biological properties of final compound. Apart from Van der Waals interactions between the MPA and IMPDH molecules, the hydrogen bonds between the lactone moiety of MPA and Gly 326 and Thr 333 of the IMPDH enzyme as well as between the phenol group of MPA and Thr 333 and Gln 441 of IMPDH also play an important role. Similarly, the *trans* configuration of the double bond in the side chain of MPA enables the interaction between its carboxylic group and Ser 276 [9], [10]. As a result, the modification of this polar carboxylic group contributed to obtaining the promising novel MPA analogs with improved therapeutic characteristics [11], [12]. MPA **1** was bonded to amino acid esters, resulting in respective amides that revealed significant antiproliferative activities [13], [14]. Additionally, the ester group in amino acid moieties might be advantageous due to better penetration through the cell membrane [14]. In our previous studies, MPA **1**was coupled to some proteinogenic amino acid esters by means of 1-ethyl-3-(3′-dimethylaminopropyl)carbodiimide (EDCI), resulting in respective amides possessing clear inhibitory activity towards IMPDH [13]. These findings encouraged us to synthesize and characterize *N*-mycophenoyl malonic acid dimethyl ester **3** (Scheme 1), which possesses a polar amide together with two ester groups at the end of the side chain. First, the attempt was made to attach amino malonic acid dimethyl ester **2** to MPA **1**with the use of EDCI, however, this approach turned out to be ineffective due to decreased nucleophilicity of the amino group in **2**. Therefore, we optimized the reaction by using propanephosphonic anhydride ($T_3P$) as a coupling agent, which has been reported to work efficiently in case of difficult amidations [15]. As a result, the desired *N*-mycophenoyl malonic acid dimethyl ester **3** was obtained, while

https://doi.org/10.1016/j.molstruc.2017.09.041

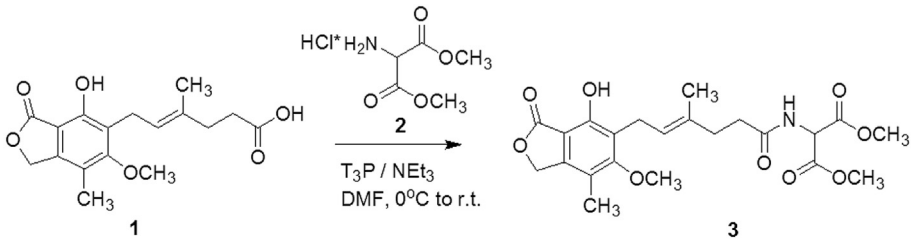


**Scheme 1.** Synthesis of *N*-mycophenoyl malonic acid dimethyl ester **3**.

the reaction yield reached 45%.

The product **3** was characterized by means of NMR and X-ray diffraction techniques. So far, the X-ray structures of the derivatives of mycophenolic acid were described for only a few species, namely, the mycophenolic acid itself [16] [17], its sodium salt [18], and mycophenolate mofetil [19].

## 2. Experimental

### 2.1. Synthesis and crystallization

The reaction was performed in dry DMF (Sigma-Aldrich), purification on silica gel 60 (230–400 mesh, Merck). $^1$H NMR and $^{13}$C NMR spectra were recorded in $CDCl_3$ on a Varian Unity 500 Plus spectrometer, while the mass spectrometry measurements were performed with an Agilent 6540 Accurate Mass Q-TOF LC/MS system using the electrospray ionisation technique. Mycophenolic acid **1** (100 mg, 0.31 mmol), dimethyl aminomalonate hydrochloride **2** (63 mg, 0.34 mmol), triethylamine (217 µl, 1.56 mmol) were dissolved in dry DMF and then cooled in an ice bath. Next, $T_3P$ solution (365 µl, 0.62 mmol, 50% in DMF, Sigma-Aldrich) was added dropwise, and the reaction mixture was stirred at room temperature overnight. Subsequently, the solvent was evaporated under vacuum, while the remaining solids were dissolved in $CH_2Cl_2$, washed with water, and dried over anhydrous $MgSO_4$. The suspension was filtered, the solvent was evaporated, and the crude product was purified via column chromatography ($CH_2Cl_2$:MeOH 100:1 to 50:1 v/v) to obtain amide **3**, with a yield of 45% (63 mg, 0.14 mmol).

Single crystals were obtained by vapor diffusion of petroleum ether into a solution of about 10 mg product **3** in 5 mL dichloromethane over 3–4 days, mp 157.0–157.7 °C.

$^1$H NMR ($\delta$ ppm): $^1$H NMR ($\delta$ ppm): 1.81 (s, 3H, $CH_3$), 2.15 (s, 3H, $CH_3$), 2.31–2.40 (m, 4H, $CH_2$), 3.39–3.40 (d, 2H, $J$ = 6.8 Hz, $CH_2$), 3.77 (s, 3H, $OCH_3$), 3.81 (s, 6H, $OCH_3$), 5.20 (s, 2H, $OCH_2$), 5.22–5.28 (m, 1H, $CH_{vinyl}$), 6.46–6.48 (d, 1H, $J$ = 6.8 Hz, CH), 7.67 (m, 1H, NH).

$^{13}$C NMR ($\delta$ ppm): 173.1, 172.6, 167.0, 163.9, 153.9, 144.3, 134.4, 123.2, 122.3, 117.0, 106.6, 70.3, 61.3, 56.2, 53.7, 35.0, 34.8, 22.8, 16.4, 11.8.

ESI—MS for $C_{22}H_{28}NO_9$ $m/z$ calculated: 450.1764, obtained: 450.1801 $[M+H]^+$, for $C_{22}H_{27}NO_9Na$ $m/z$ calculated: 472.1584, obtained: 472.1638 $[M+Na]^+$.

### 2.2. Single crystal X-ray analysis

The X-ray diffraction measurements were carried out on a relatively small crystal specimen. Data were collected on an IPDS 2T dual-beam diffractometer (STOE&Cie GmbH, Darmstadt, Germany) at 120.0(2) K with Mo-K$\alpha$ radiation of a microfocus X-ray source (GeniX 3D Mo HighFlux, Xenocs, Sassenage, France, 50 kV, 1.0 mA, $\lambda$ = 0.71069 Å). The crystal was thermostated in nitrogen stream at 120 K using CryoStream-800 device (Oxford CryoSystem, UK) during the entire experiment. Data collection and data reduction were controlled by X-Area 1.75 program [20]. The structure was solved by direct methods and refined anisotropically using the program packages WinGX2013.3 [21] and SHELX-2014 [22]. The hydrogen atoms were placed in idealized positions and refined within the riding models with the O–H bond lengths restrained to 0.84 Å and those of N–H bonds to 0.88 Å. Despite the fact that symmetry of the crystal is described by a Sohncke space group, due to the weak diffraction of the obtained specimen (conglomerate or inversion twin), the absolute configuration has not been determined during the diffraction experiment. Moreover, it has been established that the crystal contains molecules without stereogenic centers.

### 2.3. Quantum chemistry calculations

In order to study conformational stability, the potential energy surface (PES) scans obtained by means of Gaussian09W [23] at the B3LYP/6-31G theory level were used. It involved a series of energy calculations conducted for molecules with one internal coordinate (a torsion angle in our case) restricted to a set value. The scans were performed in the relaxed mode, so at every point the rest of the molecule (except for the frozen fragment) was free to adopt its optimal shape. After setting the selected value of torsion, the molecule geometry was optimized. When the molecule had attained the minimum energy level, the torsion was set to the next value (usually at an increment of 10°) and the process was repeated until the whole torsion range has been covered. Based on the collected data, the energy vs. torsion curve was plotted.

## 3. Results and discussion

*N*-mycophenoyl malonic acid dimethyl ester **3** crystallizes in the monoclinic system in the space group $P2_1$. The asymmetric unit contains one molecule, while the unit cell contains two molecules (Z = 2). The details of crystal parameters and X-ray measurements are given in Table 1 whereas the overall molecular structure of the crystal is presented in Fig. 1. The bond lengths and angles were within the expected ranges that are characteristic for the already determined structures. However, the double bond is long, *ca* 2.2% longer than the one found in **1** [17]. In this study the valence angle showing the inclination of the rigid double bond fragment and isobenzofuran ring, *i.e.* C7–C6–C5 = 111.8°, was a bit smaller than in MPA **1**, but practically the same as in the mofetil derivative [19]. The methoxy residue was directed to the same side of the isobenzofuran plane as the alkyl chain, similarly as in **1** and the sodium salt, but in a different manner than in mofetil ester (improper torsion angles C16–O9 ···C6–C5 or equivalent are 8.3; 11.9; 11.5; 14.6 and 146.0°, respectively). The internal O1–H1···O3 hydrogen bonding formed (motif S(6); see graph set analysis [24]) as in other cases, except for the sodium salt. Packing was mainly governed by the intermolecular N1–H···O4 hydrogen bonding which formed infinite chains (C(4) motif; see Ref. [24]) parallel to the crystallographic an axis (Fig. 2). These intermolecular interactions probably influence the conformation of the alkyl chain of **3**, which is a

**Table 1**
Experimental and crystallographic details for (**3**).

| | |
|---|---|
| **Crystal description** | |
| Chemical formula | $C_{22}H_{27}NO_9$ |
| $M_r$ | 449.44 |
| Crystal system, space group | Monoclinic, $P2_1$ |
| Temperature (K) | 120 |
| $a$, $b$, $c$ (Å) | 4.6755 (5), 14.0401 (9), 16.560 (2) |
| β (°) | 95.479 (9) |
| $V$ (Å$^3$) | 1082.1 (2) |
| $Z$ | 2 |
| Radiation type | Mo$K\alpha$ |
| μ (mm$^{-1}$) | 0.11 |
| Crystal size (mm) | 0.23 × 0.09 × 0.08 |
| **Data collection** | |
| Diffractometer | STOE *IPDS* 2T |
| Absorption correction | none |
| No. of measured, independent and observed [$I > 2\sigma(I)$] reflections | 11538, 3931, 2607 |
| $R_{int}$ | 0.128 |
| $(\sin\theta/\lambda)_{max}$ (Å$^{-1}$) | 0.609 |
| **Refinement** | |
| $R[F^2 > 2\sigma(F^2)]$, w$R(F^2)$, $S$ | 0.060, 0.139, 0.98 |
| No. of reflections | 3931 |
| No. of parameters | 296 |
| No. of restraints | 1 |
| H-atom treatment | H-atom parameters constrained |
| $\Delta\rho_{max}$, $\Delta\rho_{min}$ (e Å$^{-3}$) | 0.31, −0.30 |
| Absolute structure | Refined as an inversion twin |
| Absolute structure parameter | 0(2) |

Computer programs: STOE *X-AREA*, STOE *X-RED* [20], *SHELXS2014*, *SHELXL2014* [22].

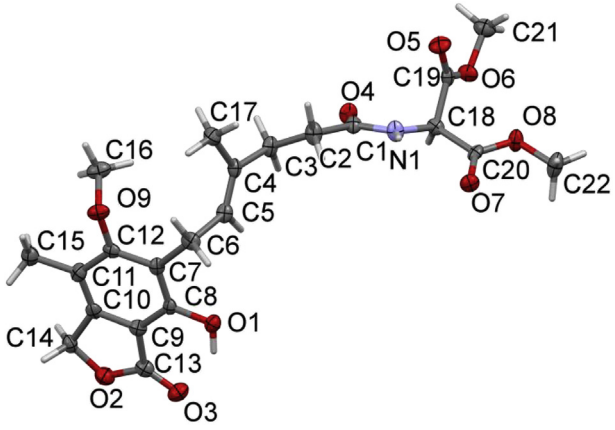


**Fig. 1.** Molecular structure of **3** showing the atom labeling scheme. The lengths (Å) of selected bonds are as follows: double bond C4–C5 1.337(9); carbonyl groups C1–O4, C13–O3, C19–O5 and C20–O7: 1.246(7), 1.199(8), 1.199(7) and 1.213(8), respectively.

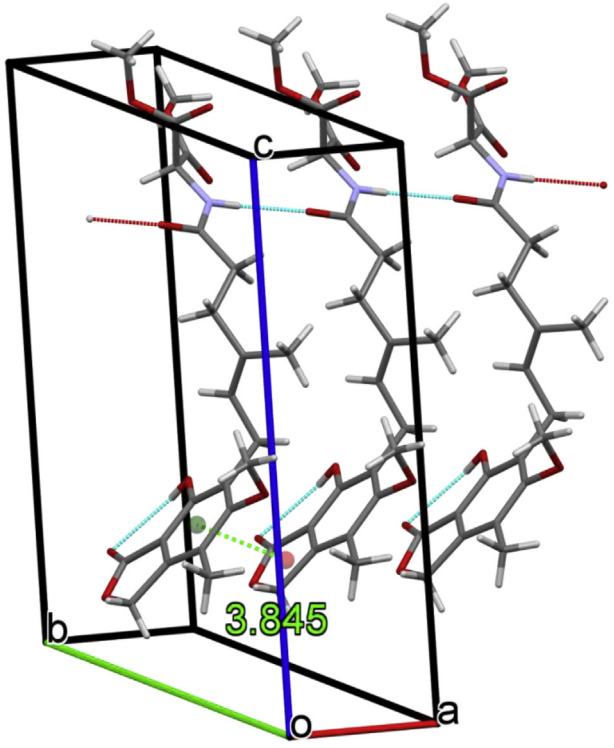


**Fig. 2.** Packing diagram for (**3**) regarding the strongest hydrogen bond donors only. The O1 hydroxyl groups form the internal cyclic hydrogen bonded $S(6)$ motif, while NH groups form infinite chains (C(4) motif)spreading parallel to the [100] direction (see the upper part of the figure). The stacking interactions are illustrated by showing the distance between centroids of the 6-membered (green) and 5-membered (red) rings. The self-assembly is reinforced by other weaker C–H···O hydrogen bonds, not shown here (see Table 2). (For interpretation of the references to colour in this figure legend, the reader is referred to the web version of this article.)

departure from the flat zig-zag form found in **1**. The full list of hydrogen bonds is given in Table 2, while the torsion angle values are listed in Table 3. Additionally, the two subrings of isobenzofuran, i.e. a 6-membered and a 5-membered one, were involved in the mutual ring stacking, with the distance between centroids of 3.845(4)Å, which is similar to that found in graphite (3.645 Å). Analogous stacking between the lactone and phenyl rings was found in the structure of the acid itself, with the distance between centroids of 3.693 Å [16]. The features of the aliphatic chains in both structures were also similar.

The side-chain conformation can be analyzed by inspecting torsion angles. A comparison of available data is presented in Table 3. It is evident that torsion at the double bond is antiperiplanar (*trans*) in all cases, and this constitutes a rigid fragment of the chain. Other torsion angles have more freedom, but only few of them are actually variable among the structures. To examine the rotational barriers in the vicinity of rigid fragments, we performed calculations for angles which are prone to change. Fig. 3 shows the barriers to rotation for torsion C2–C3–C4–C17 which define the

**Table 2**
Hydrogen-bond geometry (Å, °) for (**3**).

| *D*—H···*A* | *D*—H | H···*A* | *D*···*A* | *D*—H···*A* |
|---|---|---|---|---|
| O1—H1···O3 | 0.84 | 2.29 | 2.954 (6) | 136 |
| N1—H1*A*···O4$^{i}$ | 0.88 | 2 | 2.824 (6) | 155 |
| C14—H14*A*···O7$^{iii}$ | 0.99 | 2.48 | 3.304 (8) | 141 |
| C16—H16*B*···O1$^{iii}$ | 0.98 | 2.54 | 3.335 (7) | 139 |
| C18—H18···O7$^{ii}$ | 1 | 2.29 | 3.269 (7) | 165 |
| C22—H22*A*···O4$^{iv}$ | 0.98 | 2.44 | 3.408 (9) | 172 |

Symmetry codes: (i) $x+1, y, z$; (ii) $x-1, y, z$; (iii) $-x+2, y-1/2, -z+1$; (iv) $-x+2, y+1/2, -z+2$.

analyze the relative position of the two rigid fragments, i.e. isobenzofuran plane and the double bond fragment. Fig. 5 shows the two minima of rotation for the torsion angle C5—C6—C7—C8 at *ca* 80 and *ca* −95° separated by the barriers of an almost equal size (respectively, *ca* 5.3 and *ca* 5.8 kcal/mol for the aforementioned minima) for the above-the-ring and below-the-ring positions of the alkyl chain. The aforementioned barriers are the highest among the analyzed ones, and the conformation with both the methoxy group and alkyl chain in the *syn* position (both above the fused ring plane) is preferred.

**Table 3**
Conformation of side chains in the crystal structures of the known derivatives of **1**. Torsion angles were defined based on the compound described in this study, while for the other compounds, the equivalent angles are given.

| Torsion | MPA malonate, 3 (this study) | MPA acid 1, [16] | MPA acid ,1 [17] | NaMPA, [18] | MPA Mofetil, [19] |
|---|---|---|---|---|---|
| C1—C2—C3—C4 | 163.1(6) | 185.25 | 178.02 | −178.15 | 175,90 |
| C2—C3—C4—C5 | −110.0(7) | 5.65 | 5.78 | −98.85 | 2.36 |
| C3—C4—C5—C6 (*trans*) | 178.5(6) | 179,91 | 180.0 | 176.24 | −179.06 |
| C4—C5—C6—C7 | 127.0(7) | 120.83 | 121.91 | 135.72 | 132.89 |
| C5—C6—C7—C8 | 77.7(8) | −81.54 | −82.53 | 73.16 | 76.68 |
| C2—C3—C4—C17 | 69.8(8) | −174.35 | −172.88 | 79.70 | −176.70 |

rotation of the upper part of the chain. The diagram is not symmetrical, and it displays three minima (at *ca* −70°, *ca* 70° and *ca* 175°) separated by the energy barriers to rotation, with the two of them of a size of *ca* 1.5 and *ca* 2 kcal/mol. These rotational barriers can be easily overcome at room temperature. Also, the higher energy barriers of *ca* 4.2 and *ca* 3.5 kcal/mol are noticeable for the two possible directions of rotation. The value of C2—C3—C4—C17 torsion angle in the crystal is dependent on the intermolecular NH···O bonding.

We do not show here the energy profile of rotation for the torsion angle C2—C3—C4—C5 because it is similar to the already described profile of C2—C3—C4—C17. The only differences between these two energy profiles are the relative positions of minima since the torsion angle C2—C3—C4—C5, which equals 0°, is equivalent to the torsion angle C2—C3—C4—C17 (180°; C5 and C17 are on the opposite sides of the rigid double bond at C4).

The energy profile of rotation around the C2—C3 bond, describing the relative position of the amidomalonate residue, is shown in Fig. 4. The plot is again asymmetrical, and the energy barriers can be easily overcome at room temperature. Now, let us

The energy profile for the torsion angle C3—C4—C5—C6 is not presented here because the rotation around the double bond C4=C5 is by far less likely at room temperature. Moreover, the overlap geometry of some groups would occur during such a rotation. We also disregarded conformational changes in the malonamide part of the molecule.

## 4. Conclusions

The coupling of mycophenolic acid **1** to poor nucleophilic amines, such as aminomalonic dimethyl ester, can be approached with propanephosphonic anhydride ($T_3P$) as a coupling reagent without the necessity of protecting the phenol group in MPA **1**. The new crystal structure of compound **3** has been determined using the X-ray structural analysis, while the further characterization of the compound was performed by means of spectroscopic techniques (NMR, ESI-MS). Conformational flexibility was examined via DFT calculations, and the rotational barriers for the key fragments were determined. The observed deformation of the aliphatic chain from the flat zig-zag form was probably due to the NH···O hydrogen

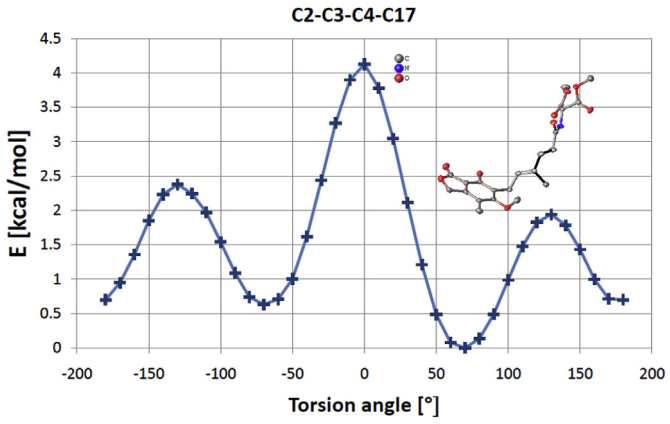


**Fig. 3.** The plot of relaxed Potential Energy Surface (PES) versus torsion angle for C2—C3—C4—C17 showing the energy barriers related to conformational changes. The torsion angle for **3** in the solid state equals 69.9(7)°. Bonds defining the examined torsion angles in the modeled molecule are shown in black.

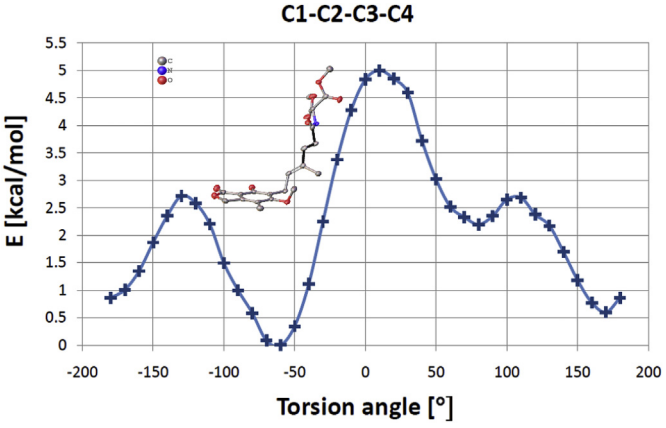


**Fig. 4.** The plot of relaxed Potential Energy Surface (PES) versus torsion angle for C1—C2—C3—C4 showing the energy barriers related to conformational changes. In the solid state, the torsion angle is 163.2(5)°. Bonds defining the examined torsion angles in the modeled molecule are shown in black.

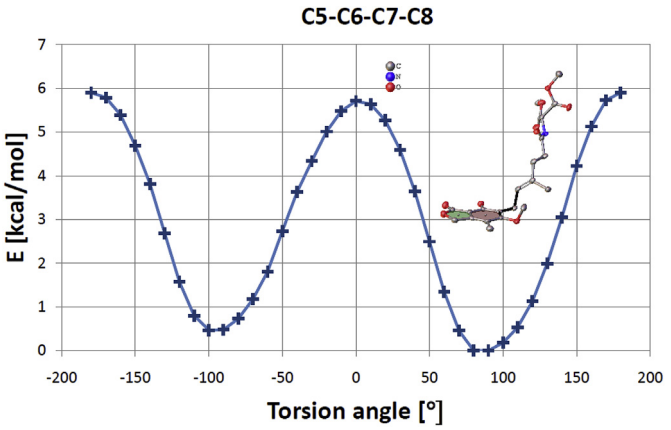


**Fig. 5.** The plot of relaxed Potential Energy Surface (PES) versus torsion angle for C5–C6–C7–C8 showing the energy barriers to rotation related to placing the alkyl chain above and below the isobenzofuran plane. The actual angle found in **3** equals 77.7(7)°. Bonds defining the examined torsion angle are shown in black.

bonds found in **3** in the solid state. Apart from the elucidation of the alkyl chain mobility at various temperatures, the results provide the parameters needed for *e.g.* Molecular Mechanics simulations. The immunosuppressive properties of the derivative **3** are presently under investigation.

## Funding

This work was financially supported by the Gdańsk University of Technology under grant DS/031946.

## Conflict of interests

None.

## Appendix ASupplementary data

Supplementary data related to this article can be found at https://doi.org/10.1016/j.molstruc.2017.09.041.

## References

[1] R. Bentley, Mycophenolic Acid: a one hundred year odyssey from antibiotic to immunosuppressant, Chem. Rev. 100 (2000) 3801–3826.
[2] G. Cholewinski, D. Iwaszkiewicz-Grzes, M. Prejs, A. Głowacka, K. Dzierzbicka, Synthesis of the inosine 5'-monophosphate dehydrogenase (IMPDH) inhibitors, J. Enzyme Inhib. Med. Chem. 30 (2015) 550–563.
[3] G. Cholewinski, M. Malachowska-Ugarte, K. Dzierzbicka, The chemistry of mycophenolic acid - synthesis and modifications towards desired biological activity, Curr. Med. Chem. 17 (2010) 1926–1941.
[4] P.H. Nelson, S.F. Carr, B.H. Devens, E.M. Eugui, F. Franco, C. Gonzalez, R.C. Havley, D.G. Loughhead, D.J. Milan, E. Papp, J.W. Patterson, S. Rouhafza, E.B. Sjogren, D.B. Smith, R.A. Stephenson, F.X. Talamas, A.-N. Waltos, R.J. Weikert, J.C. Wu, Structure–Activity relationships for inhibition of inosine monophosphate dehydrogenase by nuclear variants of mycophenolic acid, J. Med. Chem. 39 (1996) 4181–4196.
[5] N. Yang, J. Wang, Z.-W. Wang, Q.-H. Wang, H.-G. Yang, X.-J. Wang, M.-S. Cheng, Computational insights into the inhibition of inosine 5′-monophosphate dehydrogenase by mycophenolic acid analogs: three-dimensional quantitative structure–activity relationship and molecular docking studies, Chem. Biol. Drug Des. 79 (2012) 1063–1071.
[6] G. Cholewinski, D. Iwaszkiewicz-Grzes, P. Trzonkowski, K. Dzierzbicka, Synthesis and biological activity of ester derivatives of mycophenolic acid and acridines/acridones as potential immunosuppressive agents, J. Enzyme Inhib. Med. Chem. 31 (2016) 974–982.
[7] M. Malachowska-Ugarte, G. Cholewinski, K. Dzierzbicka, P. Trzonkowski, Synthesis and biological activity of novel mycophenolic acid conjugates containing nitro-acridine/acridone derivatives, Eur. J. Med. Chem. 54 (2012) 197–201.
[8] K.W. Pankiewicz, K.B. Lesiak-Watanabe, K.A. Watanabe, S.E. Patterson, H.N. Jayaram, J.A. Yalowitz, M.D. Miller, M. Seidman, A. Majumdar, G. Prehna, B.M. Goldstein, Novel mycophenolic adenine bis(phosphonate) analogues as potential differentiation agents against human leukemia, J. Med. Chem 45 (2002) 703–712.
[9] L. Hedstrom, IMP dehydrogenase: structure, mechanism, and inhibition, Chem. Rev. 109 (2009) 2903–2928.
[10] M.D. Sintchak, E. Nimmesgern, The structure of inosine 5'-monophosphate dehydrogenase and the design of novel inhibitors, Immunopharmacology 47 (2000) 163–184.
[11] W.J. Watkins, J.M. Chen, A. Cho, L. Chong, N. Collins, M. Fardis, W. Huang, M. Hung, T. Kirschberg, W.A. Lee, X. Liu, W. Thomas, J. Xu, A. Zeynalzadegan, J. Zhang, Phosphonic acid-containing analogues of mycophenolic acid as inhibitors of IMPDH, Bioorg. Med. Chem. Lett. 16 (2006) 3479–3483.
[12] D. Iwaszkiewicz-Grzes, G. Cholewinski, A. Kot-Wasik, P. Trzonkowski, K. Dzierzbicka, Investigations on the immunosuppressive activity of derivatives of mycophenolic acid in immature dendritic cells, Int. Immunopharmacol. 44 (2017) 137–142.
[13] D. Iwaszkiewicz-Grzes, G. Cholewinski, A. Kot-Wasik, P. Trzonkowski, K. Dzierzbicka, Synthesis and biological activity of mycophenolic acid-amino acid derivatives, Eur. J. Med. Chem. 69 (2013) 863–871.
[14] K. Felczak, R. Vince, K.W. Pankiewicz, NAD-based inhibitors with anticancer potential, Bioorg. Med. Chem. Lett. 24 (2014) 332–336.
[15] J.R. Dunetz, Y. Xiang, A. Baldwin, J. Ringling, General and Scalable Amide Bond formation with epimerization-prone substrates using T3P and pyridine, Org. Lett. 13 (2011) 5048–5051.
[16] W. Harrison, H.M.M. Shearer, J. Trotter, Crystal structure of mycophenolic acid, J. Chem. Soc. Perkin Trans. 2 (1972) 1542–1544.
[17] A. Covarrubias-Zuniga, N. Zuniga-Villarreal, A. Gonzalez-Lucas, J. Diaz-Dominguez, G. Espinosa-Perez, Crystal structure of mycophenolic acid: 6-(4-hydroxy-6-methoxy-7-methyl-3-oxo-1,3-dihydroisobenzofuran-5-yl)-4-methyl-hex-4-enoic acid, Anal. Sci. 16 (2000) 783–784.
[18] G. Rihs, C. Papageorgiou, S. Pfeffer, Sodium mycophenolate, Acta Crystallogr. C56 (2000) 432–433.
[19] H.S. Yathirajan, B. Nagaraj, S.L. Gaonkar, R.S. Narasegowda, P. Nagaraja, M. Bolte, Mycophenolate mofetil, Acta Crystallogr. E60 (2004) o2223–o2224.
[20] STOE &Cie GmbH, X-area 1.75, STOE &Cie GmbH, Darmstadt, Germany, 2015.
[21] L.J. Farrugia, WinGX and ORTEP for windows: an update, J. Appl. Cryst. 45 (2012) 849–854.
[22] G.M. Sheldrick, Crystal structure refinement with SHELXL, Acta Crystallogr. C 71 (2015) 3–8.
[23] [a] M. Frisch, et al., Gaussian 09, Gaussian, Inc., Pittsburgh, PA, 2009; [b] GausView03 Program Package. (www.gaussian.com/g_prod/gv5.htm).
[24] J. Bernstein, R.E. Davis, L. Shimoni, N.-L. Chang, Patterns in hydrogen bonding: functionality and graph set analysis in crystals, Angew. Chem. Int. Ed. 34 (1995) 1555–1573.